(Preprint) AAS 11-581

SOLAR RADIATION PRESSURE BINNING FOR THE GEOSYNCRHONOUS ORBIT

M.D. Hejduk[*] and R.W. Ghrist[†]

Orbital maintenance parameters for individual satellites or groups of satellites have traditionally been set by examining orbital parameters alone, such as through apogee and perigee height binning; this approach ignored the other factors that governed an individual satellite's susceptibility to non-conservative forces. In the atmospheric drag regime, this problem has been addressed by the introduction of the "energy dissipation rate," a quantity that represents the amount of energy being removed from the orbit; such an approach is able to consider both atmospheric density and satellite frontal area characteristics and thus serve as a mechanism for binning satellites of similar behavior. The geosynchronous orbit (of broader definition than the geostationary orbit—here taken to be from 1300 to 1800 minutes in orbital period) is not affected by drag; rather, its principal non-conservative force is that of solar radiation pressure—the momentum imparted to the satellite by solar radiometric energy. While this perturbation is solved for as part of the orbit determination update, no binning or division scheme, analogous to the drag regime, has been developed for the geosynchronous orbit. The present analysis has begun such an effort by examining the behavior of geosynchronous rocket bodies and non-stabilized payloads as a function of solar radiation pressure susceptibility. A preliminary examination of binning techniques used in the drag regime gives initial guidance regarding the criteria for useful bin divisions. Applying these criteria to the object type, solar radiation pressure, and resultant state vector accuracy for the analyzed dataset, a single division of "large" satellites into two bins for the purposes of setting related sensor tasking and OD controls is suggested. When an accompanying analysis of high area-to-mass objects is complete, a full set of binning recommendations for the geosynchronous orbit will be available.

INTRODUCTION

The Joint Space Operations Center (JSpOC), located at Vandenberg Air Force Base in California, is the organization responsible for performing all of the orbit determination (OD) activity necessary to maintain the US space catalogue. In order to make the OD process manageable, object are divided into groups that have similar orbit maintenance properties; this allows sensor tasking and OD parameters and controls to be set for entire groups or classes of satellites rather than for each satellite individually. The first level of class distinction is usually the overall orbit

[*] Adjunct Scientist, Mission Services Division, a.i. solutions Inc., 985 Space Center Drive, Colorado Springs, CO 80915.
[†] Principal Systems Engineer, Mission Services Division, a.i. solutions Inc., 985 Space Center Drive, Colorado Springs, CO 80915.

type, with the high-level distinctions of low-earth orbit (LEO), highly-eccentric orbit (HEO), middle-earth orbit (MEO), and geosynchronous orbit (GEO);* but subsequent subdivisions are typically based on the non-conservative forces that affect the orbit, as these are usually the most difficult to model and thus govern the settings for the OD process. In the LEO and many HEO orbits, the most significant non-conservative force is atmospheric drag; and a notable amount of effort has been applied in the last decade to developing better class divisions regarding the amount of atmospheric drag a particular satellite is expected to experience.[1,2] For the geosynchronous orbit, the principal modeled non-conservative force is that due to solar radiation pressure. While the precision OD theory in use at the JSpOC includes a solar radiation pressure model and solution, at present this datum is not used in a systematic way to bin or divide geosynchronous objects in order to optimize GEO catalogue maintenance. The purpose of the present investigation is to determine whether there are some simple differentiations, based on satellite solar radiation pressure susceptibility, that can be articulated and serve as a basis for separating GEO objects for sensor tasking and OD control purposes.

This investigation will first begin with an examination of the much more carefully studied atmospheric drag problem in LEO (and HEO). It will be useful to understand the general manner in which this non-conservative force has been parameterized in order to define useful satellite bins, and the magnitude of the accuracy differences that justified the introduction of a new bin should be applicable to the problem in GEO. Second, the solar radiation pressure problem proper will be confronted to determine an analogous construct to the atmospheric drag case that can be used as a GEO non-conservative force characterizer. Third, the particular case of GEO rocket bodies will be examined to determine, for this more circumscribed object type, whether object divisions by solar radiation pressure susceptibility are durable in themselves and whether such divisions map to tracking and OD-related outcomes, such as resultant vector accuracy. Fourth, all of the non-stabilized main catalogue satellites in GEO will be examined as a group to see whether natural divisions into bins suggest themselves under this viewing. Finally, the more "problematic" object type of high area-to-mass ratio (HAMR) objects will be included in the analysis in order to help to assemble an overall recommendation for geosynchronous object binning.

LEO NON-CONSERVATIVE FORCE AND THE ENERGY DISSIPATION RATE

The retarding force on a satellite due to atmospheric drag is given as[3]

$$\ddot{r} = -\frac{1}{2} C_D \frac{A}{M} \rho v_r^2 e_v \ , \tag{1}$$

in which *r*-double-dot is the anti-velocity acceleration, C_D is the drag coefficient (dimensionless), A is the spacecraft frontal area (normal to the velocity vector), M is the spacecraft mass, ρ is the atmospheric density, v_r is the magnitude of the velocity relative to the atmosphere, and e_v is the unit vector in the direction of the spacecraft velocity. Because the spacecraft mass and frontal area are generally not known, the group quantity of $C_D A/M$ is solved for as a unit and called the ballistic coefficient. The ballistic coefficient gives some insight into the behavior of the satellite in the presence of atmospheric drag; however, it does not represent the overall effect on the satel-

* The definitions of these four main orbital regime divisions in use at the JSpOC, are as follows:
LEO: period < 225 minutes
HEO: period >= 225 minutes and eccentricity > 0.3
MEO: 600 < period <800 minutes and eccentricity > 0.3
GEO: 1300 < period <1800 minutes, eccentricity <0.3, and inclination <35 degrees

lite's orbital behavior because the atmospheric density, which will vary substantially with the orbit characteristics, is not included. A more comprehensive measure is needed to represent the entire effect of this non-conservative force.

EDR Definition and History

Barker *et al.* confronted the problem of characterizing the effect of atmospheric drag on an orbit while performing a study for the Omitron Corporation to determine the relationship between tracking density and resultant vector accuracy.[1,2] As a single-parameter encapsulation of the effect of atmospheric drag, they proposed the construct of the instantaneous energy dissipation rate (EDR), given the formal definition of

$$EDR(t) = -\vec{A}_D \bullet \vec{V}\,, \tag{2}$$

in which A_D is the inertial drag acceleration vector and V is the inertial velocity vector. This quantity (in watts/kg) represents the amount of energy being removed from the orbit due to atmospheric drag (or, occasionally, being brought to the orbit through other processes). A single numerical value for EDR for a given OD solution is an averaged value calculated over the orbit determination interval. This construct thus represents the whole of the retarding force in a single (albeit averaged) quantity.

Based on the results of their investigation, Omitron proceeded to divide the orbital population into eleven EDR bins, each of which would represent a different level of severity for the atmospheric drag retarding force. Table 1 provides a list of these bin boundaries and the percent of the satellite catalogue (all object types) assigned to each bin. As these bins have been used both operationally and in simulation environments, it has emerged that for some applications it is acceptable to aggregate some of the bins, namely bins 2-4, 5-7, and 8-10, in order to reduce the number of different categories to manage.[4] These aggregated categories are enumerated and formally defined at the bottom of Table 1. It is noteworthy that 90% of the objects appear in bins 0 and 1 (those for no drag and very low drag); only 10% of the catalogue appears in the more highly delineated bins 2-10 (or the three aggregated bins at bottom).

Table 1. Energy Dissipation Rate (EDR)

EDR Bin	Lower W/kg Value	Upper W/kg Value	% of Catalogue (May 2007)
0	0	0	15.5
1	0+	0.0006	72.7
2	0.0006	0.0010	2.6
3	0.0010	0.0015	1.5
4	0.0015	0.0020	0.8
5	0.0020	0.0030	1.2
6	0.0030	0.0060	2.0
7	0.0060	0.0090	1.0
8	0.0090	0.0150	0.8
9	0.0150	0.0500	0.8
10	0.0500	0.0500+	1.1
2-4	0.0006	0.0020	4.9
5-7	0.0020	0.0090	4.2
8-10	0.0090	0.0500+	2.7

Accuracy Ratios among EDR Bins

Because solar radiation pressure does not act consistently in the anti-velocity direction, it is clear that the EDR construct cannot be used to characterize SRP effects. However, what can be transferred from the EDR construct is the differences in performance between different bins that led the Omitron analysts to choose to define the bins as they did. Any solar-radiation-pressure-related bin definitions should remain consistent with the drag-related binning in terms of the significance of different bin definitions. Because two different types of EDR bins are presently in service (the full eleven from the original report and the aggregated reduction to five), it is important to characterize the significance of moving among bins in both the finer and coarser instantiations.

The authors concluded that the best way to determine the significance of moving from one bin to another is to characterize the average state vector error for the satellites in each bin and therefore be able to state the significance of bin-changes in terms of accuracy decrement. Fortunately, the JSpOC operational system contains a robust vector accuracy assessment algorithm, which constructs reference orbits for each object and compares each object's state vector to the object's reference orbit in order to characterize the vector's propagation error.[5] A database of these accuracy data for 2010 was available for the present study. To address releasability issues, all accuracy data in this paper have been multiplied by an arbitrary constant and are presented without axis labels. Because the focus of the original Omitron study supported a set of operational adjustments in order to maximize the OD accuracy at the 72-hour prediction point, it seems natural to choose the accuracy data for that particular propagation point to investigate the significance, from an accuracy perspective, in moving from one EDR bin to another.

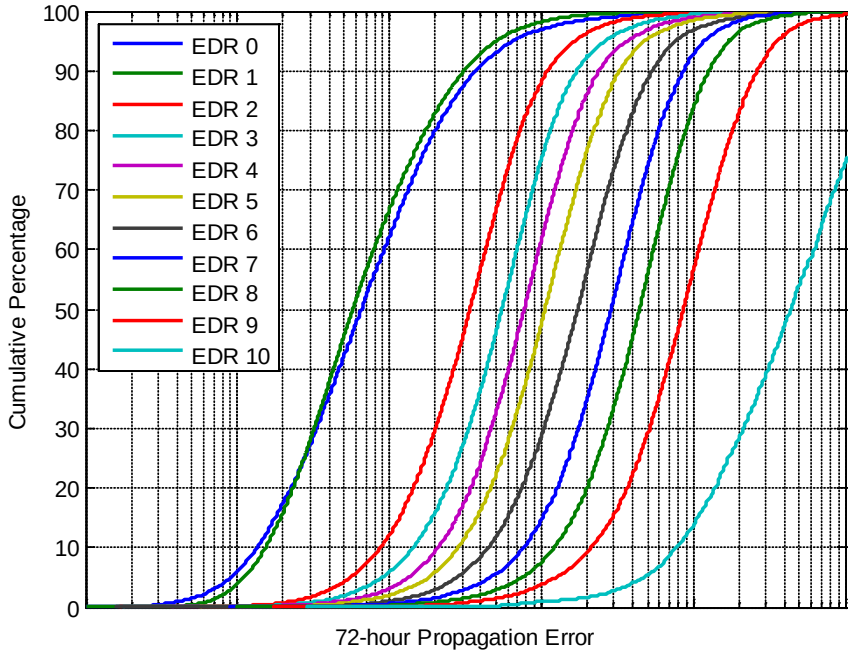

Figure 2a: CDF Plots of 72-hour Propagation Error by EDR Bin, for Fine Divisions (log plot)

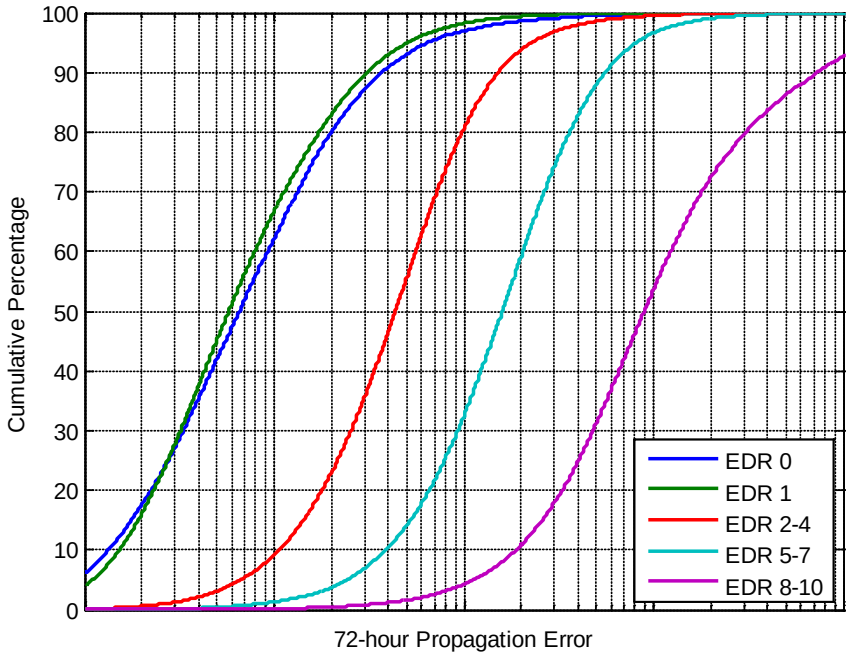

Figure 2b: CDF Plots of 72-hour Propagation Error by EDR Bin, for Coarse Divisions (log plot)

Figures 2a and 2b provide cumulative distribution function (CDF) plots of the accuracy distribution for the eleven smaller-granularity EDR bins and the five amalgamated EDR bins. In both cases, bins 0 and 1 address a part of the catalogue outside of the major binning and were set aside; similarly, bin 10 represents the very highest drag regime (with no upper limit to the size of the EDR value that it can contain) and were set aside as well. In looking at the remaining CDFs, one can observe that the separation (in log space) between the CDFs is approximately the same. This suggests there is a single scalar by which one could multiply each CDF in order to produce the CDF to its immediate right.

Taking the 50th percentile for the CDFs for EDR bins 2-9, calculating the multiplier needed to make each CDF into its right-hand neighbor, and averaging these values results in an average multiplier value of 1.7. Applying this process to the data in Figure 2b (made somewhat more difficult by the paucity of usable curves), the emergent factor is 4.6.

Admittedly, this is not the most robust procedure for determining the significance level associated with bin sizes; but it does provide some general parameters to apply to the solar radiation pressure investigation: minor divisions in solar-radiation-pressure-related binning should reflect a multiplicative difference in accuracy of about 1.7, and major divisions should reflect a multiplicative difference of about 4.6.

GEO NON-CONSERVATIVE FORCE: SOLAR RADIATION PRESSURE

The acceleration of a spacecraft due to the application of solar radiation pressure is given by the following relationship[3]

$$\ddot{\vec{r}} = -P_s C_R \frac{A}{M} \frac{\vec{r}_s}{r_s^3} \ , \tag{3}$$

in which P_s is the solar radiation pressure in the vicinity of the Earth (usually in units of watts-seconds per cubic meter), C_R is the radiation pressure coefficient (which essentially defines the

absorptivity of the satellite's construction materials), A is the effective area of the satellite's surface exposed to the solar radiation, M is the spacecraft's mass, r_s is the distance to the sun, and $\vec{r}_s$ is the unit vector from the satellite to the sun. In examining this equation, one can see in the grouping of C_R, A, and M a similar construct to the ballistic coefficient; because in the first treatments of the subject (see reference 6) the symbol used to represent C_R was the Greek letter γ, this ballistic-coefficient-like quantity is called AGOM (Area-[times]-Gamma-Over-Mass).

As pointed out earlier during the discussion of atmospheric drag, because the atmospheric density ρ varies with object perigee height and actual flight path through the atmosphere, it is not sufficient to examine the ballistic coefficient alone to determine the magnitude of the effect of this non-conservative force on a given satellite. For the case of solar radiation pressure, however, the situation is ameliorated by the relative constancy of the P_s and r_s terms. While the P_s term does vary seasonally by about 3% due to the eccentricity of the earth's orbit and the distance to the sun does change slightly as the GEO object moves through its daily orbit, the effect of these phenomena is dwarfed by the other imprecisions in the solar radiation pressure solution, namely satellite attitude changes, the umbral/penumbral model to determine the degree of satellite illumination, and the varying absorptivity of the satellite materials. It is thus adequate, certainly to first-order and probably well beyond that, to use the AGOM value as a measure of the effect of solar radiation pressure on geosynchronous satellites.

PROOF-OF-CONCEPT: GEO ROCKET BODIES

There are over one hundred rocket bodies in the geosynchronous orbit. The great majority of these are of the SL-12 family (a workhorse Russian rocket body), but there are enough multiple examples of other types that this group of satellites constitutes a good test set: rocket bodies are a somewhat circumscribed set of shapes yet with different dimensions, surface materials, and space aging effects. If systematic differences can be seen among the AGOM values for different rocket body types, and if these differences can be linked to similar differences in vector accuracy, then the contention that AGOM can serve as a separator among objects in the main catalogue is strengthened.

To explore this postulation for GEO rocket bodies and to extend the examination to other object types, an operational data capture was conducted. AGOM solutions for all of the main-catalogue GEO objects for the period of January through September 2010 were captured and made available for analysis. Accuracy data for these objects, from the same database mentioned in this paper's section on energy dissipation rate, was also made available, allowing an examination of the relationship between AGOM and vector propagation error. Finally, although no accuracy data were available for these objects, the AGOM histories for about forty GEO HAMR objects were also captured to serve as an overall point of comparison.

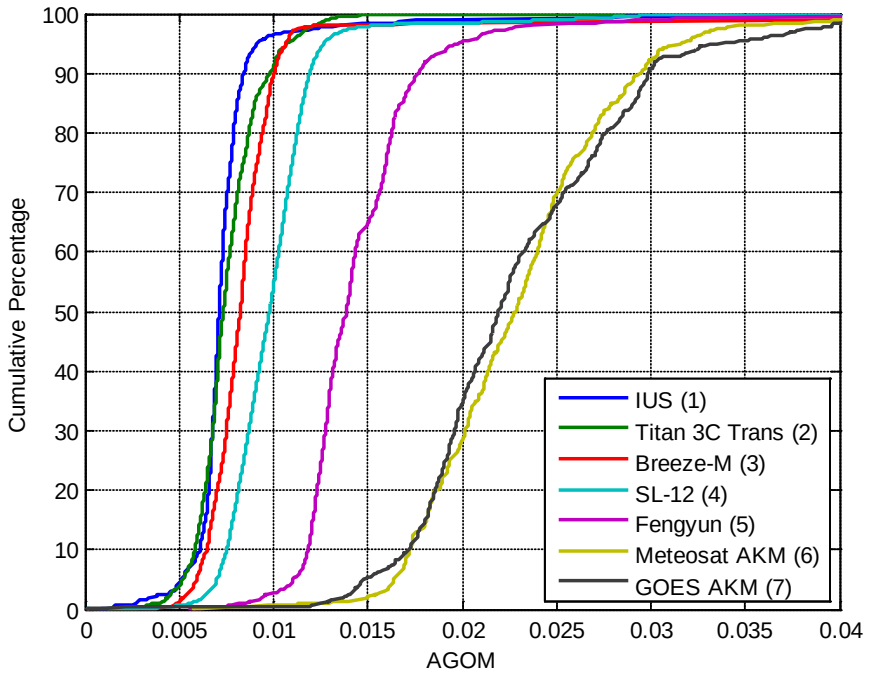

Figure 3: CDF Renderings of AGOM Values for Different Rocket Body Types

Figure 3 shows the AGOM distributions for the most populated types of GEO rocket bodies. For ease of reference, each of the CDF lines in the graph in Figure 3 is assigned a sequence number 1-7, working from left to right at the 70% line on the graph; these numbers are also given in the legend. The plot suggests three distinct groups: The four most leftward curves [1-4], the lone curve in the middle [5], and the two together at the far right [6-7]. These groups may appear visually separate, but it is better to confirm such a result with a statistical test than to rely exclusively on graphical perception. To this end, a two-tailed *t*-test (equal means; equal but unknown variances) was run against various groupings of the above rocket body types. The formal hypothesis test for the situation is the following:

H_0: The two groups are drawn from the same parent (Gaussian) distribution[*]
H_1: The two groups come from different parent distributions

If the *p*-value associated with a particular *t*-test is small, it indicates that the null hypothesis (H_0) is unlikely to be true and thus counsels the rejection of the null hypothesis in favor of the research hypothesis (H_1). A summary of the test results is given in Table 2 below, which is to be read in concert with Figure 3.

Table 2: *t*-test Results for AGOM Values of Different Rocket Body Families

Grouping	*p*-value	Comment
[1 2 3] vs [4]	0.57	Keep H_0; part of same group
[1 2 3 4] vs [5]	0.08	Could go either way but lean toward keeping H_0
[1 2 3 4 5] vs [6 7]	1.27E-11	Reject H_0; [6] and [7] from different populations

[*] The number of AGOM samples for each satellite typically ranged between 100 and 300, so the datasets under analysis here are large enough that the *t*-test should give durable results even if the overall population is not strictly Gaussian.

These results lend support to keeping rocket body group [1 2 3 4] together, to separating group [6 7] from the rest, and to leaving type [5] as a "fielder's choice" as to whether it be subsumed with group [1 2 3 4] or set apart as its own unit.

This latter issue is clarified somewhat by examining the 72-hour vector propagation error data for these groups, as represented in Figure 4. There is very little difference between group [1 2 3 4] and type [5] but a significant difference between either of those groups and group [6 7] (red line). At the 50th percentile, the ratio of the "red" group accuracy value to that of the "blue" and "green" families exceeds the ratio for a minor EDR division (1.7) but does not reach the level for a major EDR division (4.6). At the least, therefore, the AGOM differences between these two groups ([1 2 3 4 5] vs [6 7]) do point to a palpable accuracy difference, on the model of the differences between EDR bins in the drag regime. The present exercise with rocket bodies thus shows that differences in AGOM should be explored as a general method of setting tracking and maintenance parameters for satellites in GEO.

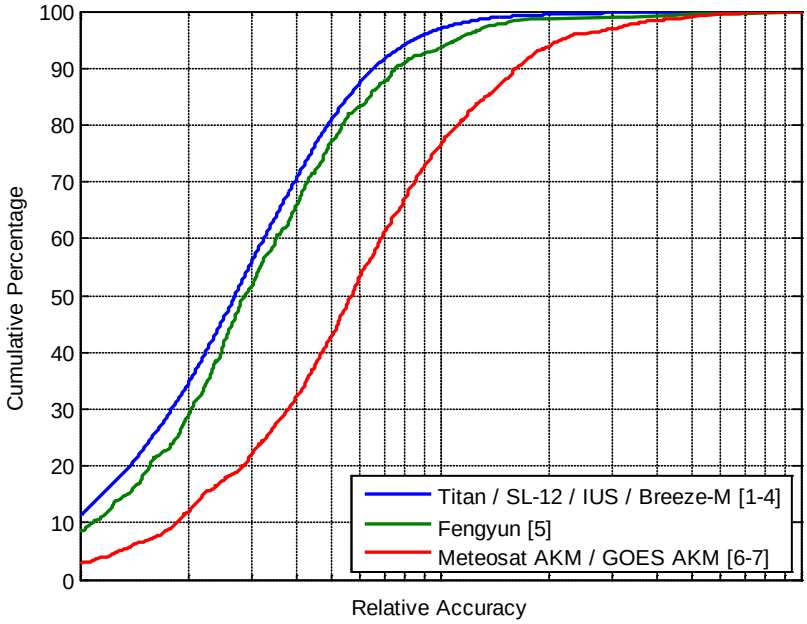

Figure 4: 72-hour Vector Propagation Error for Three Rocket Body Groups

ROCKET BODIES AND NON-STABILIZED PAYLOADS

The next analytical step is to add non-stabilized payloads to the investigation, and the most illustrative presentation when more than one object type is involved is an accuracy versus AGOM (specifically median AGOM versus median accuracy for each object) scatter plot. Figure 5 provides such a plot, giving results for both the rocket body data previously discussed and for non-stabilized GEO payloads. Stabilized GEO payloads execute frequent station-keeping maneuvers in order to maintain their longitudinal position; and as many of these small maneuvers get included in the OD updates, the resultant accuracy data for this object type are not fully reliable, especially in comparison to that of objects that do not experience thrust-related dynamics changes. It is thus best to limit consideration to rocket bodies and non-stabilized payloads. For the purposes of this study, the latter have been defined as having a drift rate greater than or equal to 0.03 degrees of longitude per day.

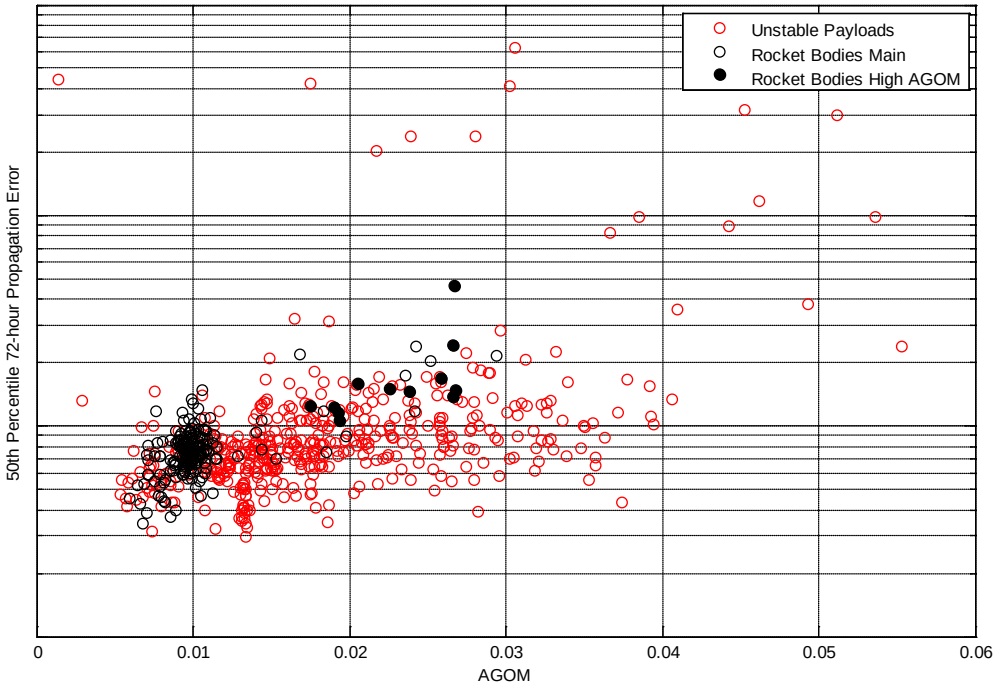

Figure 5: Vector Propagation Error vs AGOM for Rocket Bodies and Unstable Payloads

In Figure 5, the black circles are the rocket bodies analyzed in the previous section; and one can see that they are a well-behaved group on the whole (occupying for the most part a distinct cluster). The filled black circles are the Meteosat and GOES rocket bodies; and it is clear that these inhabit both a different AGOM region and a different accuracy level. The red circles represent unstable payloads. Some of these have smaller vector errors despite somewhat larger AGOM values; but on the whole the average AGOM value is higher, and vector errors on the whole increase as AGOM increases. Additionally, more "outlier" satellites manifest themselves in this group, with vector errors one to two orders of magnitude larger than those for the GEO rocket bodies.

Figure 6 is a re-presentation of these same data but with some additions. The blue squares represent the median value of the vector errors for all data within ± 0.025 in AGOM of each square's location, and the blue line is a least-squares fit of the blue squares. In moving from the AGOM values of 0.01 to 0.03, the relative vector error increases from about six units to about ten units, which meets the 1.7 multiplier threshold (from the EDR bin analysis) for defining a new bin; so there is good justification to divide the dataset into at least two bins. For such division(s), it is acceptable, and in fact desirable, to consider natural groupings as presented in the plot rather than an *a priori* formulary that might not be responsive to the actual situation. Certainly the main grouping of rocket bodies and the high-AGOM rocket bodies should be in different groupings, which would suggest a dividing line somewhere between 0.012 and 0.017 in AGOM. One can also observe an uptick in high-vector-error objects at an AGOM value of about 0.015; it would seem best to keep these in the same group rather than divide them right at a bin boundary. There is additionally a group of low-error unstable payloads at an AGOM level of about 0.013; these should stay with the lower-error group. A dividing line that conforms to all of these criteria can be drawn at an AGOM value of 0.014, and the green line on the graph represents this boundary.

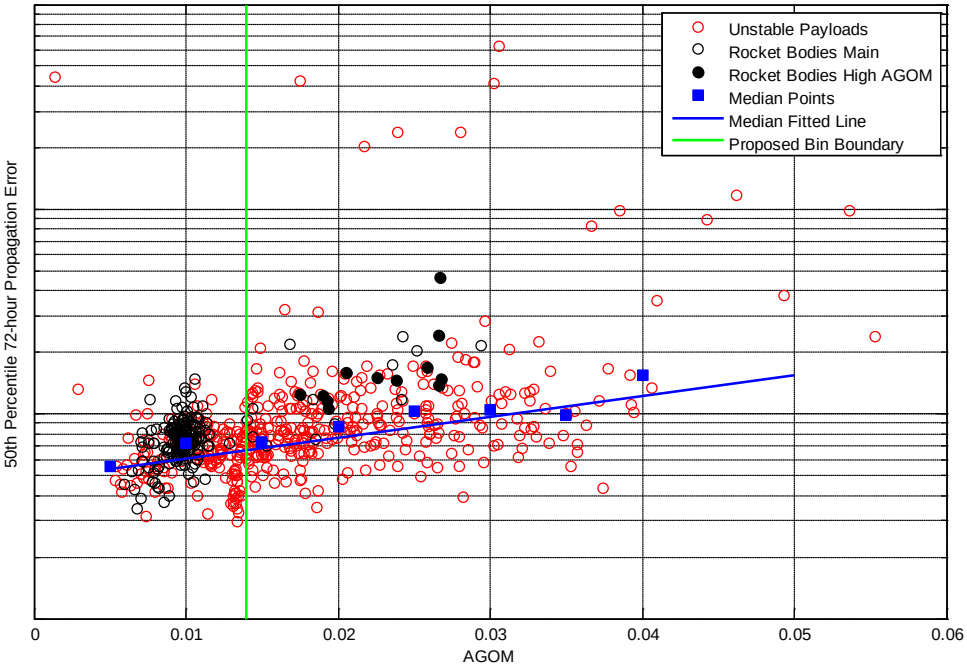

Figure 6: Vector Propagation Error vs AGOM, with Additions

One could consider a second division at an AGOM value of 0.04, for at AGOM values greater than this point the "main" part of the unstable payload distribution disappears, leaving only satellites with much larger vector errors. However, spacecraft with similar errors are observed at the lower AGOM values as well; so the justification for creating a separate bin for these few objects is not very strong.

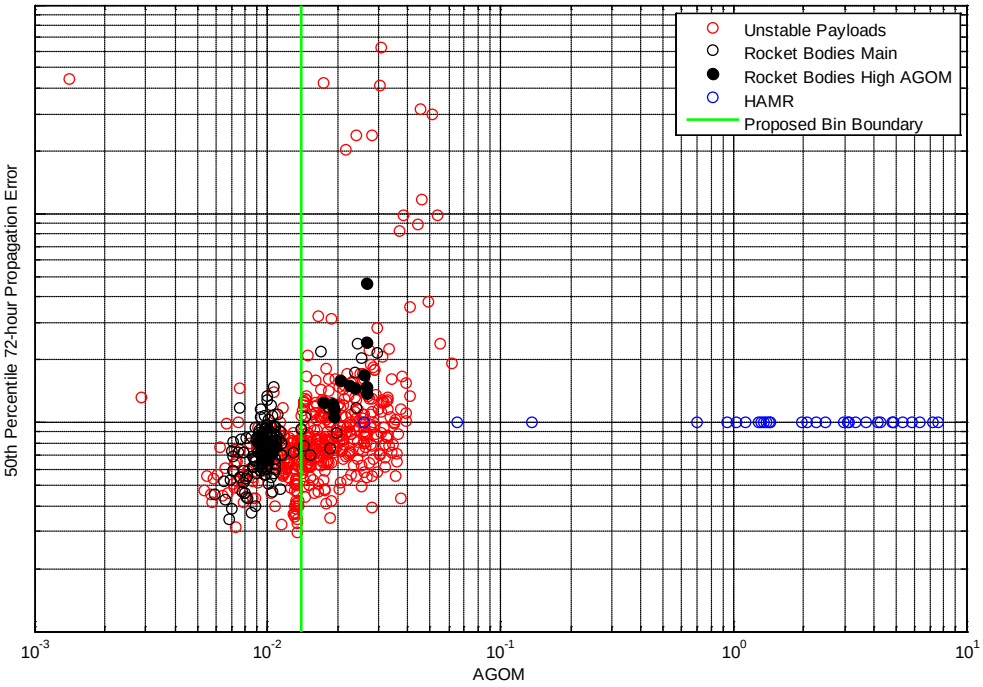

Figure 7: Vector Propagation Error vs AGOM, with HAMR Objects

HIGH AREA-TO-MASS RATIO (HAMR) OBJECTS

Some data on a set of approximately forty HAMR objects in GEO were made available for this study. Unfortunately, accompanying vector error data were not available, so the present effort could not extend its binning recommendations to that group of satellites; but some heuristic conclusions can be drawn. Figure 7 includes the AGOM values for this set of objects (with a null accuracy value) so that they may be seen in contrast to the other datasets examined. Clearly, these satellites come from a population vastly different from the other objects; and one would indeed expect them to merit their own separate sensor tasking and OD controls. Lacking accuracy information, however, it is not possible to determine what subdivisions within this group would be appropriate.

CONCLUSIONS AND FUTURE WORK

In examining the rocket bodies and non-stabilized payloads, a division of these objects into two bins based on an AGOM threshold of 0.014 is justified by the data and in keeping with the binning paradigm used for atmospheric drag. HAMR objects differ significantly from this dataset in terms of AGOM value and, one expects, in terms of vector propagation error as well. The next leg of this analysis will examine these objects in detail, as well as considering whether use of an object size criterion, such as RCS or visual magnitude, is helpful to the vector error prediction as well. At that point, a comprehensive set of binning recommendations for the GEO orbit regime can be assembled.

ACKNOWLEDGMENTS

This paper was supported by the National Aeronautics and Space Administration Goddard Space Flight Center (NASA/GSFC), Greenbelt, MD, under the Flight Dynamics Support Services (FDSS) contract (NNG10CP02C), Task Order 30. The authors wish to thank David Pauls of AFSPC/A9A and Lauri Newman of NASA/GSFC for underwriting this research, as well as Karen Richon of NASA/GSFC for her helpful comments and suggestions.

REFERENCES

[1] Barker, W. *et al.* "Integrated Space Command and Control: Space Surveillance Network Optimization (SSNO) Study." Lockheed-Martin Technical Report #B001-3.1.4-SSNO-RPT-01, 23 AUG 2002.

[2] Barker, W. *et al.* "Integrated Space Command and Control: Space Surveillance Network Optimization (SSNO) Study Extension." Lockheed-Martin Technical Report #B001-5.7.4-SSAC2-lb_le_lf-RPT-02, 31 OCT 2003.

[3] Montenbruck, O. and Gill, E. *Satellite Orbits: Models, Methods, and Applications*. Berlin: Springer Verlag, 2005.

[4] Hejduk, M.D. "Space Catalogue Accuracy Modeling Simplifications." *Proceedings of the 2008 AAS Astrodynamics Specialists Conference*. Honolulu, HI. August 2008.

[5] Hejduk, M.D., Ericson, N.L., and Casali, S.J. "Beyond Covariance: A New Accuracy Assessment Approach for the 1SPCS Precision Satellite Catalogue." 2006 MIT / Lincoln Laboratory Space Control Conference, Bedford, MA. May 2006.

[6] Koskela, P. E. "Orbital Effects of Solar Radiation Pressure on an Earth Satellite." *The Journal of the Astronautical Sciences*, IX, 3, 1962.